

Quantum imaging

L.A. Lugiato, A. Gatti and E. Brambilla

Istituto Nazionale per la Fisica della Materia, Dipartimento di Scienze Chimiche Fisiche e Matematiche, Università dell'Insubria, Via Valleggio 11, 22100 Como, Italy

We provide a brief overview of the newly born field of quantum imaging, and discuss some concepts that lie at the root of this field.

I. PREAMBLE

This article is based on the plenary talk that one of us (L.A.L.) gave at the ICSSUR Conference in Boston in June 2001.

The starting point is provided by the general topic of the spatial aspects of quantum optical fluctuations. This has been the object of several studies in the past, but only recently there has been a constant focus of attention, which is mainly due to the fact that the spatial features may open new possibilities, e.g. in the direction of parallel processing and multichannel operation by quantum optical procedures. Once realized that these studies may have interesting perspectives, it is natural to coin a new name as quantum imaging to designate this field.

This article includes an introductory part, in which we discuss few concepts that play a key role in this field, such as the intrinsic connection between quantum entanglement and squeezing, the spatial squeezing and the near field/far field duality. Next, we discuss several topics in the field of quantum imaging and illustrate recent ideas and results. The topics include

- Detection of weak phase and amplitude objects beyond the standard quantum limit,
- Amplification of weak optical images preserving the signal-to-noise ratio (noiseless amplification),
- Entangled two-photon microscopy,
- Quantum limits in the detection of small displacements and in image reconstruction,
- Quantum lithography,
- Quantum teleportation of optical images.

Several of the results and approaches that we will illustrate have been pursued by the participants in the European Project QUANTIM (Quantum Imaging), that started in January 2001.

II. INTRODUCTION

A. Intrinsic connection between squeezing and quantum entanglement

One might consider that squeezing is a rather old-fashioned field, whereas for entanglement one immediately thinks of such topics as quantum computing, or quantum teleportation, or cryptography, and concludes that it is a new and exciting field. However one must remark that, in the framework of the continuous variable approach, squeezing and quantum entanglement are intrinsically linked, they are basically two faces of the same phenomenon. This circumstance explains by the way why a series of meetings entitled Squeezed States and Uncertainty Relations is still gathering so many people.

In order to demonstrate this point in details, let us consider two radiation beams and the associated annihilation operators of photons a_1 and a_2 , and let us focus on the simple linear transformation to another couple of beams b_1 and b_2 :

$$b_1 = \frac{a_1 + a_2}{\sqrt{2}}, \quad b_2 = \frac{a_1 - a_2}{\sqrt{2}} \quad (1)$$

This transformation can be implemented very easily. If, for example, a_1 and a_2 have the same frequency and the same polarization, it is realized by a 50/50 beam splitter. If they have the same frequency but horizontal and vertical polarization, respectively, one can use a polarizing beam splitter in which the two output beams are polarized at 45° and 135° , respectively.

Now, the general result for transformation (1) is that

- if a_1 and a_2 are EPR (Einstein-Podolski-Rosen [1]) entangled beams with respect to quadrature components, then beams b_1 and b_2 are squeezed with respect to two orthogonal quadrature components and, vice versa,
- if a_1 and a_2 are squeezed beams with respect to two orthogonal quadrature components, b_1 and b_2 are EPR entangled beams with respect to quadrature components.

To prove this result, let us consider the interaction Hamiltonian for parametric down-conversion in the nondegenerate configuration and in the approximation of classical undepleted pump [2]

$$H = ig\alpha \left(a_1^\dagger a_2^\dagger - a_1 a_2 \right) \quad (2)$$

where g is the coupling constant and α is the classical amplitude of the pump beam. As it is well known, in the nondegenerate configuration the two beams a_1 and a_2 are entangled both with respect to photon number and with respect to two quadrature components [2–4]. The entanglement can be explicitly shown by applying the time evolution operator corresponding to the Hamiltonian (2) to the uncorrelated vacuum state, for an interaction time τ_{int}

$$e^{-\frac{i}{\hbar} H \tau_{int}} |0\rangle_1 |0\rangle_2 = \sum_{n=0}^{\infty} c_n |n\rangle_1 |n\rangle_2$$

$$c_n = \frac{[\tanh(g\tau_{int}/\hbar)]^n}{\cosh(g\tau_{int}/\hbar)}. \quad (3)$$

Clearly the state described by Eq.(3) is not factorizable, and implies perfect correlation between the photon number in the two beams.

If we now introduce into Eq. (2) the expression of a_1 and a_2 as a function of b_1 and b_2

$$a_1 = \frac{b_1 + b_2}{\sqrt{2}}, \quad a_2 = \frac{b_1 - b_2}{\sqrt{2}}, \quad (4)$$

we obtain immediately the alternative expression

$$H = i\frac{g\alpha}{2} \left[\left(b_1^\dagger \right)^2 - b_1^2 \right] - i\frac{g\alpha}{2} \left[\left(b_2^\dagger \right)^2 - b_2^2 \right], \quad (5)$$

which corresponds to the sum of two interaction hamiltonians for parametric down-conversion in the degenerate configuration. Hence the beams b_1 and b_2 are squeezed, and, because of the minus sign in front of the second term, the squeezing is in orthogonal quadrature components. For example, when α is real b_1 is squeezed with respect to the Y quadrature (imaginary part of the annihilation operator) and b_2 is squeezed with respect to the X quadrature (real part of the annihilation operator).

B. Spatially multimode versus singlemode squeezing

In almost all literature on squeezing one considers singlemode squeezing. If one wants to detect a good level of squeezing, the local oscillator must be matched to the squeezed spatial mode and, in addition, it is necessary to detect the whole beam. If one detects only part of the beam the squeezing is immediately degraded, because a portion of a mode necessarily involves higher order modes, in which squeezing is absent. What we can call *local squeezing*, i.e. squeezing in small regions of the transverse plane, can be obtained only in presence of *spatially multimode squeezing*, i.e. squeezing in a band of spatial modes. This has been predicted by Sokolov and Kolobov for the traveling wave optical parametric amplifier (OPA) [5,6] and by our group for the optical parametric oscillator (OPO) [7,8].

Let us dwell a moment, for example, on the case of the OPA (Fig.1a), in which one has a slab of $\chi^{(2)}$ material which is pumped by a coherent plane wave of frequency $2\omega_s$. A fraction of the pump photons are down-converted into signal-idler photon pairs, which are distributed over a broad band of temporal frequencies around the degenerate

frequency ω_s . For each fixed temporal frequency, the photon pairs are distributed over a band of spatial frequencies labeled by the transverse component \vec{q} of the wave vector.

If, in addition to the pump field, we inject a coherent plane wave with frequency ω_s and transverse wave vector \vec{q} (Fig. 1b), in the output we have a signal wave which corresponds to an amplified version of the input wave and for this reason the system is called optical parametric amplifier. Because of the pairwise emission of photons, there is also an idler wave which, close to degeneracy, is symmetrical with respect to the signal wave.

Referring to the case in which only the pump is injected, two regimes can be distinguished. One is that of pure spontaneous parametric down-conversion, as in the case of a very thin crystal. In this case coincidences between partners of single photon pairs are detected. The other is that of dominant stimulated parametric down-conversion, in which a large number of photon pairs at a time is detected. In the following we will consider both cases alternatively.

C. Near field/Far field duality

We want to illustrate the key spatial quantum properties of the field emitted by an OPA, in the linear regime of negligible pump depletion, or by an OPO below threshold. In the OPA case, we consider the configuration of a large photon number.

In the near field (see Fig. 2) one has the phenomenon of spatially multimode squeezing or local squeezing discussed in Sec. II B. A good level of squeezing is found, provided the region which is detected has a linear size not smaller than the inverse of the spatial bandwidth of emission in the Fourier plane. If, on the other hand, one looks at the far field (which can be reached, typically, by using a lens as shown in Fig.2) one finds the phenomenon of *spatial entanglement* between small regions located symmetrically with respect to the center. Precisely, if one considers two symmetrical pixels 1 and 2 (Fig.3), the intensity fluctuations in the two pixels are very well correlated or, equivalently, the fluctuations in the intensity difference between the two pixels are very much below the shot noise [9,10]. Because this phenomenon arises for any pair of symmetrical pixels, we call it spatial entanglement. The same effect occurs also for quadrature components, because in the two pixels the fluctuations of the quadrature component X are almost exactly correlated, and those of the quadrature component Y are almost exactly anticorrelated [11]. The minimum size of the symmetrical small regions, among which one finds spatial entanglement, is determined by the final aperture of optical elements, and is given, in the paraxial approximation, by $\lambda f/a$, where λ is the wavelength, f is the focal length of the lens and a is the aperture of optical elements (e.g. the lens aperture)(Fig. 2). In a more realistic model of the OPA, the finite waist of the pump field should be taken into account. In this case the minimum size of the regions where entanglement is detectable in the far field is mostly determined by the pump waist.

The spatial entanglement of intensity fluctuations in the far field is quite evident even in single shots (the pump field is typically pulsed). Fig. 4a shows a numerical simulation in a case of non collinear phase matching at degenerated frequency. One observes the presence of symmetrical intensity peaks, which become broader and broader as one reduces the waist of the pump field. A similar situation is observed in an experiment performed using a LBO crystal [12]. We observe finally that the near field/far field duality can be understood on the basis of the intrinsic connection between squeezing and quantum entanglement. The spatial entanglement in the far field arises from the correlation between the modes $a_{\vec{q}} \sim \exp[i\vec{q} \cdot \vec{x}]$ and $a_{-\vec{q}} \sim \exp[-i\vec{q} \cdot \vec{x}]$, , which in the far field give rise to two separated and opposite spots in the transverse plane (\vec{q} is the transverse wave vector and \vec{x} is the position vector in the transverse plane).

On the other hand, in the near field there is no squeezing in modes $a_{\vec{q}}$ and $a_{-\vec{q}}$ separately, whereas there is large squeezing in the combination modes and $b_{\vec{q}} = (a_{\vec{q}} + a_{-\vec{q}})/\sqrt{2}$ and $b_{-\vec{q}} = (a_{\vec{q}} - a_{-\vec{q}})/\sqrt{2}$, which annihilate photons on spatial modes $\sim \cos(\vec{q} \cdot \vec{x})$ and $\sim \sin(\vec{q} \cdot \vec{x})$. In the near field it is possible to observe this squeezing by using a local oscillator with a $\cos(\vec{q} \cdot \vec{x})$ or $\sin(\vec{q} \cdot \vec{x})$ spatial configuration [7]. One notices immediately that the relation between modes $a_{\vec{q}}$, $a_{-\vec{q}}$ and modes $b_{\vec{q}}$, $b_{-\vec{q}}$ coincides with Eq. (1), which, as we have seen, transforms entangled beams into squeezed beams, and viceversa.

III. TOPICS IN QUANTUM IMAGING

Next we focus specifically on studying the quantum aspects of the very classical field of imaging. We will discuss several topics in order.

A. Detection of weak amplitude or phase objects beyond the standard quantum limit

Let us consider first the case of a weak amplitude object which is located, say, in the signal part of the field emitted by an OPA (Fig.5). Both signal and idler are very noisy and therefore, in the case of large photon number, if the object is weak and we detect only the signal field, the signal-to-noise ratio for the object is low. But, because of the spatial entanglement, the fluctuations in the intensity difference between signal and idler are small. Hence if we detect the intensity difference, the signal-to-noise ratio for the object becomes much better. This scheme is conceptually related to well known ‘ghost image’ experiments [13,14] in the regime of detection of single photon pairs.

Next, let us pass to the case of a weak phase object in which one can exploit, instead, the property of spatially multimode squeezing. The configuration is the standard one of a Mach-Zender interferometer in which, as it is well known, one can detect a small phase shift with a sensitivity beyond the standard quantum limit by injecting a squeezed beam in the port through which usually normal vacuum enters. If we have a weak phase image (Fig.6) we can obtain the same result by injecting a spatially multimode squeezed light [15].

B. Quantum imaging with entangled photon pairs

This approach has been formulated by Abouraddy, Saleh, Sergienko, and Teich for the regime in which single photon pairs are detected. They have shown that using entangled photons in an imaging system offers possibilities that cannot be attained when entanglement is absent [16].

In a classical imaging configuration one has a source, an illumination system, an object, an imaging system and a detector. The field at the detection plane is related to that at the object plane by a linear integral transformation with a kernel h . Let us focus on the interesting case illustrated in Fig. 7, in which the imaging is performed using photon pairs, in which case the topography of the system allows for two branches with different kernels to be simultaneously illuminated, a system that was heuristically considered by Belinskii and Klyshko [17]. The two-photon wave function is denoted $\psi(\vec{x}, \vec{x}')$ (\vec{x} and \vec{x}' are source position vectors in the transverse plane) and the two kernels are denoted h_1 and h_2 for the signal and idler beams 1 and 2, respectively. Next, let us introduce two assumptions. The first is that the two photons are entangled. This is expressed by the fact that the wave function ψ includes a factor $\delta(\vec{x} - \vec{x}')$, which expresses the fact that the two photons are generated at the same point. The second assumption is that the first photon is detected by a bucket detector, which can reveal its presence, but not at all its location. On the other hand, the other detector is capable of scanning the position of the photon, and one detects the coincidences between photon pairs. The key point is that in this situation the probability distribution for the position of the second photon depends not only on h_2 but also on h_1 , and this is true even though the position of photon 1 is not detected. Thus, suppose that, for example, there is nothing in the path of photon 2, whereas in the path of photon 1 there is an object which may be transmissive/reflective, diffusive or scattering (see Fig.7). By using a bucket detector for the first photon, and by scanning the position of the second photon and detecting coincidences one can obtain an image of the object which is in the path of the first photon despite the fact that the position of this photon is not scanned. The essential point is that, when the two photons are entangled, such distributed quantum imaging is in general partially coherent, and can possibly be fully coherent in which case phase information about the object is preserved, whereas for classically correlated but unentangled photons the imaging would be incoherent. These authors have also applied the principle of entangled-photon imaging to quantum holography [16].

C. Entangled two-photon microscopy

In recent years there has been a lively interest in entangled-photon microscopy [18].

The surge in the development of fluorescence microscopy based on two-photon excitation using laser light has been driven by the principal advantages of this technique over single-photon excitation: a pair of low-energy photons can deposit as much energy as a single ultraviolet photon thereby exciting a fluorescent molecule within a sample with greater penetration depth, better resolution, and less risk of damage upon absorption along the optical path. However, in order to obtain two-photon absorption with a classical light source such as a laser, a very large photon-flux density is necessary to place two photons within a small enough volume and time window so that the fluorescent molecule can absorb them. In this latter case, a femtosecond-pulsed high-power laser is used directly as the source of light, which can produce undesired photodamage of the specimen.

On the other hand, entangled photons generated by the process of spontaneous parametric downconversion in a nonlinear crystal comprise intrinsically paired photons within a small volume and short time window. In principle, therefore, far smaller photon-flux densities can be used to effect absorption so that the risk of photodamage to the

specimen is reduced (see Fig. 8). Yet other possible advantages arise from the direct proportionality of absorption to photon-flux density (rather than the quadratic relation that holds for ordinary two-photon absorption) and the fact that the sum of the photon energies of each entangled pair is a constant and equal to the energy of the downconverted pump photon whereas the sum energy is far broader for photons from a femtosecond laser). However, one of the principal challenges in implementing this form of microscopy is obtaining an entangled-photon flux that is sufficient to excite two-photon transitions, which have a limited cross section [19].

D. Image amplification by parametric down conversion

Let us come back to the configuration of Fig. 1b in the case of a large number of photon pairs. Let us assume that now, instead of a plane wave at frequency close to ω_s , we inject a coherent monochromatic image (Fig.9) of frequency ω_s . Parametric image amplification has been extensively studied from a classical viewpoint (see e.g. [12]). A basic point in Fig.9 is that, if the image is injected off axis, one obtains in the output a signal image, that represents an amplified version of the input image, and also a symmetrical idler image. An interesting situation arises if one has, in addition to the amplifier, a pair of lenses located at focal distances with respect to the object plane, to the amplifier and to the image plane (Fig.10). As it was shown by our group [9,11,20], in the limit of large amplification the two output images can be considered twin of each other even from a quantum mechanical viewpoint. As a matter of fact, they do not only display the same intensity distribution but also the same local quantum fluctuations. Precisely, let us consider two symmetrical pixels in the two images (Fig.11). It turns out that the intensity fluctuations in the two pixels are identical, i.e. exactly correlated/synchronized. On the other hand, the phase fluctuations are exactly anticorrelated. Hence the situation with respect to phase and intensity fluctuations is similar to what one obtains by breaking a fossil in two parts (Fig. 12). In fact the two parts have the same ‘intensity’, if one establishes an analogy between intensity and thickness, but they have opposite phase, since one is clockwise and the other anticlockwise, one is convex and the other concave. So in this way, from one image one obtains twin images in a state of spatial entanglement which involves also the quadrature components X and Y , as it was already described in the case of pure parametric fluorescence without any signal injection in Sec.II C.

There is, however, a negative point that concerns the signal-to-noise ratio. When the input image is injected off axis, this mechanism of amplification is phase insensitive and therefore, as it is well known, it adds 3 dB of quantum noise in the output [21]. In order to have noiseless amplification, i.e. amplification which preserves the signal-to-noise ratio, one must inject two coherent images symmetrically (Fig.13) [20]. In this case one has in the input two identical, but uncorrelated images and in the output two amplified images in a state of spatial quantum entanglement. One can prove that this symmetrical configuration is phase sensitive and, in fact, as it was shown in [22,23] the amplification can become noiseless. A couple of years ago there was a landmark experiment by Kumar and collaborators [24] which demonstrated the noiseless amplification of a simple test pattern.

E. Measurement of small displacements

This topic has been recently studied from a quantum mechanical standpoint by Fabre and his group [25]. They analyze the displacement of a light beam. According to the Rayleigh diffraction limit, the position of the beam can be measured with an error on the order of the beam section. However, one can use, rather, a split detector which measures the intensities i_1 and i_2 from the two halves of the beam cross section (Fig.14).

If one displaces gradually the beam with respect to the detector and plots the intensity difference, one obtains a curve like that shown in Fig.14 and the precision in the measurement of the displacement is limited only by noise. The standard quantum limit is given [26] by the ratio of the Rayleigh limit to the square root of the photon number. In this way one can measure shifts in the sub-nanometer range. In the case of the microscopic observation of biological samples, one cannot raise the photon number and therefore it is important to have the possibility of going beyond the standard quantum limit by reducing the noise in the intensity difference $i_1 - i_2$ below the shot noise level. To achieve this, a possibility is to use a beam in a state of spatial entanglement between its upper and its lower part, because in this way the number of photons in the two parts is basically the same and the fluctuations in the intensity difference are very small. Another possibility, which was proposed in [25], is to synthesize a special two-mode state which arises from the superposition of a Gaussian mode in a squeezed vacuum state and a spatially antisymmetrical mode which lies in a coherent state. The antisymmetrical mode is obtained from a Gaussian mode by flipping upside down one of the two halves. One shows that in this way one can measure displacements beyond the standard quantum limit. Experiments with this configuration are presently conducted in the laboratory of Bachor at the University of Canberra in collaboration with the group of Fabre [27].

F. Image reconstruction

Kolobov and Fabre have recently studied the quantum limits in the process of image reconstruction [28]. The very well known scheme they analyzed is shown in Fig.15. The object is contained in a finite region of size X . The imaging system is composed by two lenses and an aperture. Because of the transverse finiteness of the imaging system, diffraction comes into play, with a consequence that some details of the object are blurred. In order to better reconstruct the object, one can proceed as follows. One considers the linear operator H which transforms the object into the image, its eigenvalues and its eigenfunctions, which are called prolate spheroidal functions:

$$Hf_n(\vec{x}) = \mu_n f_n(\vec{x}) \quad (6)$$

If the imaging were perfect, H would be the identity operator and all eigenvalues would be equal to unity. An imperfect imaging introduces a sort of loss so that $\mu_n \leq 1$. Now one expands the image $e(\vec{x})$ on the basis of the eigenfunctions:

$$e(\vec{x}) = \sum_n c_n f_n(\vec{x}) \quad (7)$$

and obtains the coefficients c_n . The object $a(\vec{x})$ is reconstructed by the following expression

$$e(\vec{x}) = \sum_n \frac{c_n}{\sqrt{\mu_n}} f_n(\vec{x}) \quad (8)$$

where the coefficients c_n have been replaced by $c_n \sqrt{\mu_n}$.

In principle the reconstruction is perfect, but a problem is introduced by the circumstance that when the index n is increased the eigenvalues μ_n quickly approach zero. As it is shown in [28], this feature makes the reconstruction of fine details very sensitive to noise, so that again quantum noise represents the ultimate limitation. The idea proposed in [28] is to illuminate the object by bright squeezed light instead of coherent light, and to replace the vacuum state in the part of the object plane outside the object itself by squeezed vacuum radiation. In this way one can obtain a definite improvement of the resolution in the reconstruction, beyond the standard quantum limit.

G. Quantum optical lithography

This topic was pioneered by Scully and Rathe [29] and has become a focus of attention after the theoretical paper by Dowling and collaborators [30]. In this work there are two key points (Fig. 16). First, the entangled photon pairs emitted by an OPA in a regime of pure parametric down-conversion are conveyed to a 50/50 beam splitter, and second the lithographic interference pattern is obtained by two-photon absorption. The effect is that the wavelength of the interference modulation is halved with respect to the standard one-photon absorption pattern. This is due to the fact that, according to a well known experiment by Hong and Mandel [31], the entangled photons emerge from the beam splitter either in pair on the upper side or in pair on the lower side of the beam splitter, and there is never a coincidence between one photon on each side. It is just the quantum interference between the two possible two-photon paths which produces the halved interference pattern. A very recent experiment by Shih and collaborators [32], related to this configuration, provides a first-principle demonstration of quantum lithography and exhibits nicely the halving effect in the passage from one-photon to two-photon absorption. A recent article [33] considers, instead of the regime of single photon pairs detection, the case in which the OPA produces a large number of photons pairs. It shows that in this limit the halving effect is well preserved, even if the fringe visibility is reduced by a factor 5. A simple interpretation of the halving effect in this case is obtained by observing that the two entangled beams emitted by the OPA are transformed by the beam splitter into a pair of squeezed beams (see Sec.II A), and therefore one detects the two photon absorption of the interference of two squeezed vacuum fields. In Fig. 17 we see the squeezing ellipses of the two beams. One of the two ellipses rotates with respect to the other corresponding to the variation of the phase χ (see Fig.16) which represents the phase difference among the two paths. Clearly it is not necessary to perform a rotation of 2π . to return to the initial configuration. A rotation of π is enough, and this produces the halving of the wavelength. This consideration suggests an alternative procedure to attain an experimental demonstration of the principle of optical lithography: the interference of two vacuum squeezed beams produced by two optical parametric oscillators below threshold which share the same pump beam.

As it is well known, a minimum uncertainty squeezed vacuum state has the form [2]

$$\exp \left[\zeta a^2 - \zeta^* (a^\dagger)^2 \right] |0\rangle \quad (9)$$

where ζ is a c-number and $|0\rangle$ is the vacuum state. One can generalize the argument above by considering a state of the form

$$\exp\left[\zeta a^N - \zeta^* (a^\dagger)^N\right]|0\rangle \quad (10)$$

which can be obtained, for example, by a material with a χ^N nonlinearity, in which a single pump photon is down-converted into N entangled photons. One can consider the interference of two beams, one of which is in state (10), while the other lies in the state

$$\exp\left[\zeta (ae^{i\chi})^N - \zeta^* (a^\dagger e^{-i\chi})^N\right]|0\rangle \quad (11)$$

obtained from (10) by a rotation of the angle χ which corresponds to the phase difference between the two paths plus, possibly, a constant. Clearly, a rotation of $\frac{2\pi}{N}$ is enough to return to the initial configuration and as a consequence the wavelength of the interference pattern, detected by N-photon absorption, is reduced by a factor N. Of course, this argument does not predict the visibility of the fringes.

H. Quantum teleportation of optical images

As a final futuristic point, let us consider the quantum teleportation of optical images [34]. In this case we consider an OPA without any input image. Nonetheless in the output we have two twin images which are very noisy but still in a state of spatial entanglement, and are sent one to the station of Alice and the other to the station of Bob. The teleportation scheme generalizes the one formulated by Vaidman, Braunstein and Kimble [35,36] for quantum teleportation in terms of continuous variables. The input image to be teleported lies in an arbitrary quantum state and using a 50/50 beam splitter it is combined with one of the two noisy twin images, so that its quantum state is completely corrupted at this stage. However, the system as a whole works as a quantum fax machine which is capable of reproducing in the output image not only the average properties of the input image, but also the details of its quantum state. This is due to the fact that, thanks to the perfect correlation between the two noisy entangled twin images, all the noise introduced at the initial state is exactly cancelled in the final stage. This process is called ‘holographic quantum teleportation’ because it shows striking analogies with standard holography, apart from the fact that, of course, it works on a quantum level.

ACKNOWLEDGMENTS

We thank Claude Fabre, Mikhail Kolobov, Eric Lantz, Bahaa Saleh, Alexander Sergienko, Malvin Teich for giving us permission of including in this paper material provided by them. This work is supported by the European FET Project QUANTIM (Quantum Imaging).

REFERENCES

-
- [1] Einstein A., Podolsky B. and Rosen N., Phys.Rev. 47, 777 (1935)
 - [2] Walls D.F. and Milburn G., *Quantum Optics* (Springer-Verlag, Berlin 1994); Scully M.O. and Zubairy M.S., *Quantum Optics* (Cambridge University Press 1997); Schleich W. *Quantum Optics in Phase Space* (Wiley VCH, 2001) ; Barnett S.M. and Radmore P.M., *Methods in Theoretical Quantum Optics* (Clarendon Press Oxford 1997)
 - [3] Reid M.D. and Drummond P.D., Phys. Rev. Lett. 60, 2731 (1988); Reid M.D., Phys. Rev. A 40, 913 (1989)
 - [4] Ou Z.Y., Pereira S. F., Kimble H.J. and Peng K.C., Phys. Rev. Lett. 68, 3663 (1992); Ou Z.Y., Pereira S.F. and Kimble H.J., Appl.Phys.B 55, 265 (1992)
 - [5] Kolobov M.I. and Sokolov I.V., Sov.Phys JETP 69, 1097 (1989); Phys.Lett.A 140, 101 (1989); Europhys.Lett. 15,271 (1991)
 - [6] Kolobov M.I., Rev. Mod. Phys. 71, 1539 (1999)

- [7] Lugiato L.A. and Gatti A., Phys.Rev. Lett. 70, 3868 (1993); Gatti A. and Lugiato L.A., Phys. Rev. A 52, 1675 (1995); Lugiato L.A., Brambilla M. and Gatti A., Optical Pattern Formation, in *Advances in Atomic, Molecular and Optical Physics*, vol. 40, 229 (Academic Press, Boston 1999)
- [8] Lugiato L.A. and Grangier Ph., J. Opt. Soc. Am. B 14, 225 (1997)
- [9] Gatti A., Brambilla E., Lugiato L.A. and Kolobov M.I., Phys. Rev. Lett. 83, 1763 (1999)
- [10] Brambilla E., Gatti A., Lugiato L.A. and Kolobov M.I., Eur. Phys. J. D **15**, 127 (2001)
- [11] Navez P., Brambilla E., Gatti A. and Lugiato L.A., Spatial entanglement of twin quantum images, Phys. Rev. A., in press
- [12] Devaud F. and Lantz E., Eur. Phys. J. D 8, 117 (2000); Lantz E. and Devaud F., Numerical simulation of spatial fluctuations in parametric image amplification, Eur. Phys. J. D, in press (2001).
- [13] Strekalov V., Sergienko A.V., Klyshko D.N., and Shih Y.H., Phys.Rev.Lett. 74,3600 (1995)
- [14] Barbosa G.A.,Phys.Rev.A 54,4473 (1996)
- [15] Kolobov M.I. and Kumar P., Opt. Lett. 18, 849 (1993)
- [16] Saleh B.E.A., Abouraddy A.F., Sergienko A.V., and Teich M.C., Phys. Rev. A 62, 043816 (2000); Abouraddy A.F., Saleh B.E.A., Sergienko A.V., and Teich M.C., Phys. Rev. Lett. 87, 123602 (2001); Abouraddy A.F., Saleh B.E.A., Sergienko A.V., and Teich M.C., Optics Exp. 9, 498 (2001); Abouraddy A.F., Saleh B.E.A., Sergienko A.V., and Teich M.C., Entangled-photon Fourier optics, J. Opt. Soc. Am. B 19, in press (2002)
- [17] Belinskii A.V. and Klyshko D.N., Sov. Phys. JETP 78, 259 (1994)
- [18] Teich M.C. and Saleh B.E.A., Československý časopis pro fyziku (Prague) 47, 3 (1997)
- [19] H.-B. Fei, B. M. Jost, S. Popescu, B. E. A. Saleh, and M. C. Teich, Phys. Rev. Lett. 78, 1679 (1997)
- [20] Gatti A., Brambilla E., Lugiato L.A. and Kolobov M.I., J.Opt. B Quantum Semiclass.Opt. 2, 196 (2000)
- [21] Caves C.M., Phys. Rev. D 26, 1817 (1982)
- [22] Kolobov M.I. and Lugiato L.A., Phys Rev. A 52,4930 (1995)
- [23] Sokolov I.V., Kolobov M.I. and Lugiato L.A., Phys. Rev. A 60, 2420 (1998)
- [24] Choi S.-K., Vasilyev M. and Kumar P., Phys.Rev. Lett. 83, 1938 (1999)
- [25] Fabre C., Fouet J.B., and Maitre A., Opt. Lett. 25,76 (2000)
- [26] Treps N., Effets quantiques dans les images optiques, doctoral thesis at Universite Paris VI, 2001
- [27] Fabre C. private communication
- [28] Kolobov M.I. and Fabre C., Phys. Rev.Lett. 85, 3789 (2000)
- [29] Rathe U.V. and Scully M.O., Lett. Math. Phys. 34, 297 (1995)
- [30] Boto A.N., Kok P. Abrams D.S., Braunstein S.L., Williams C.P. and Dowling J.P., Phys.Rev.Lett. 85, 2733 (2000)
- [31] Hong C.V. and Mandel L., Phys.Rev. A 31, 2409 (1985)
- [32] D'Angelo M., Ceckhova M.V. and Shih Y.H., Two-photon diffraction and quantum lithography, preprint quant-ph/0103035
- [33] Agarwal G.S., Boyd R.W., Nagasako E.M. and Butley S.O., Phys. Rev. Lett. 86, 1389 (2001)
- [34] Sokolov I.V., Kolobov M.I., Gatti A. and Lugiato L.A., Opt. Comm. 193,175 (2001)
- [35] Vaidman L., Phys.Rev.A. 49, 1973 (1994)
- [36] Braunstein S.L. and Kimble H.J., Phys.Rev. Lett. 80, 869 (1998)

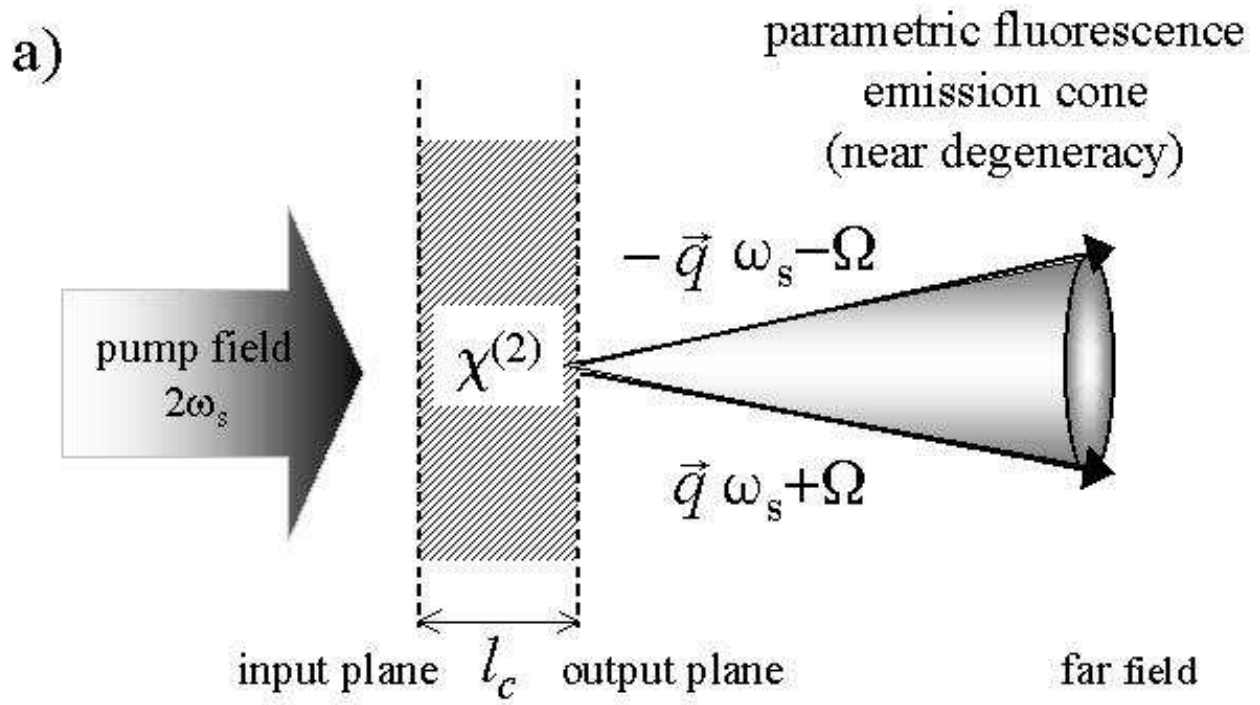


Fig.1 (a) Scheme for parametric down-conversion.

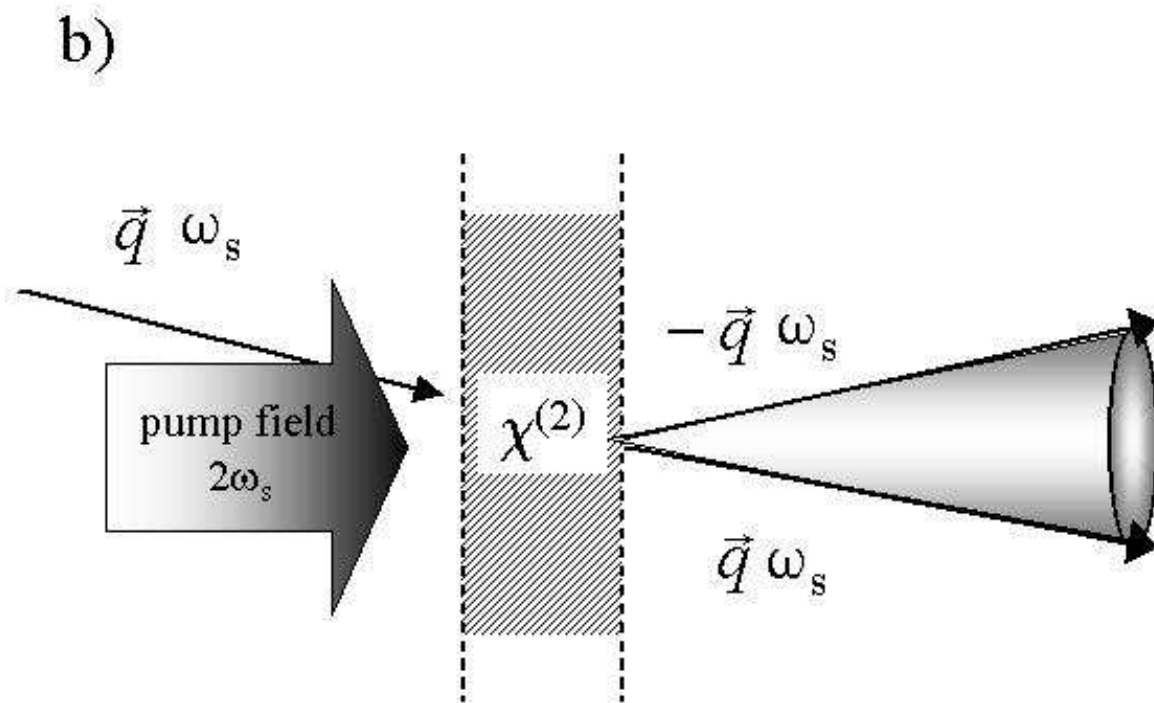


Fig 1.(b) Parametric amplification of a plane wave. \vec{q} is the component of the wave-vector in the planes orthogonal to the pump propagation direction.

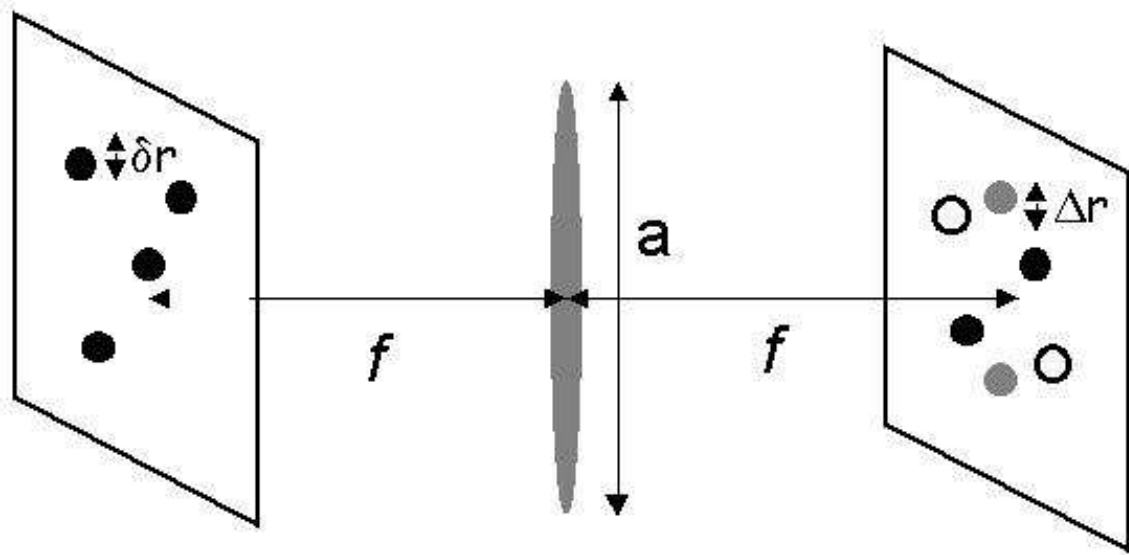


Fig.2. Illustration of the near field/far field duality. f is the focal length of the lens.

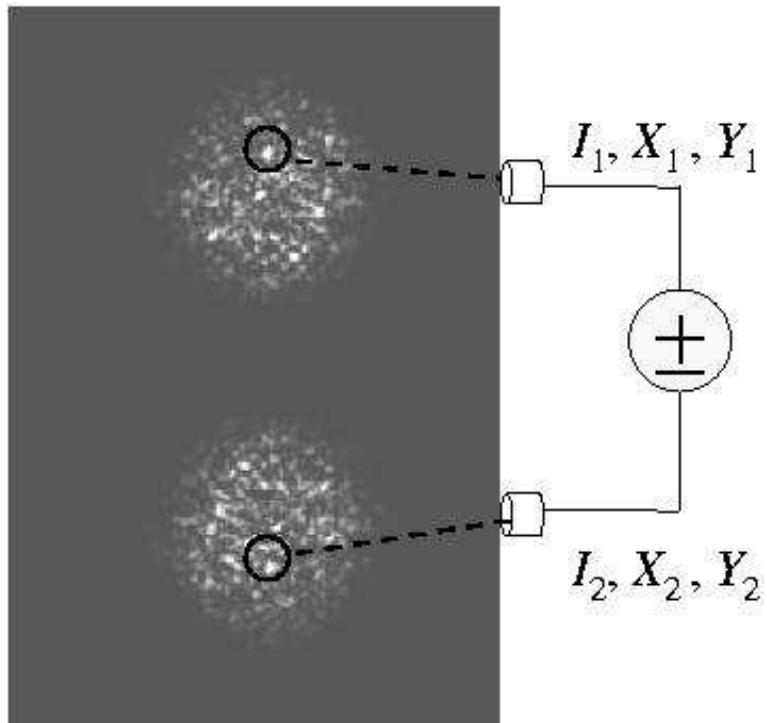


Fig.3. Illustration of the concept of spatial entanglement. I_i, X_i, Y_i ($i = 1, 2$) denote the intensities and the quadrature components measured in the two pixels 1 and 2, respectively.

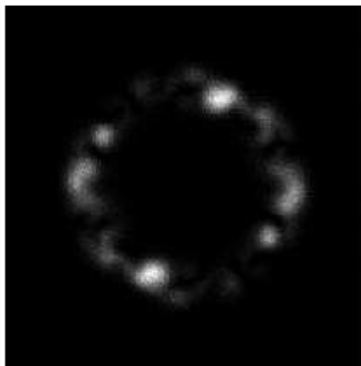
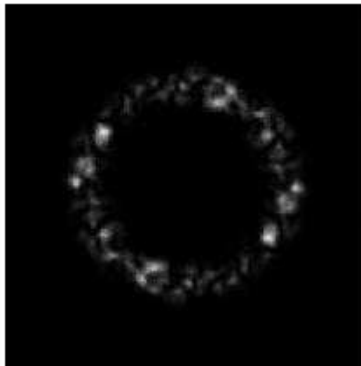
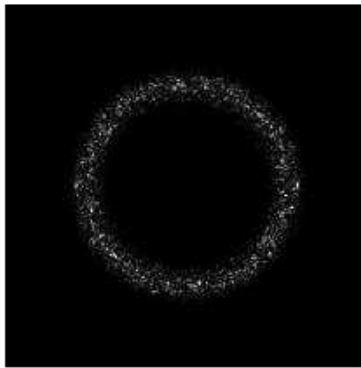


Fig.4 (a) Intensity distribution in the far field for a single shot of the pulsed pump field. a) Numerical simulations. The waist of the pump beam is $1000 \mu\text{m}$, $300 \mu\text{m}$, $150 \mu\text{m}$ in the three frames from top to bottom, respectively.

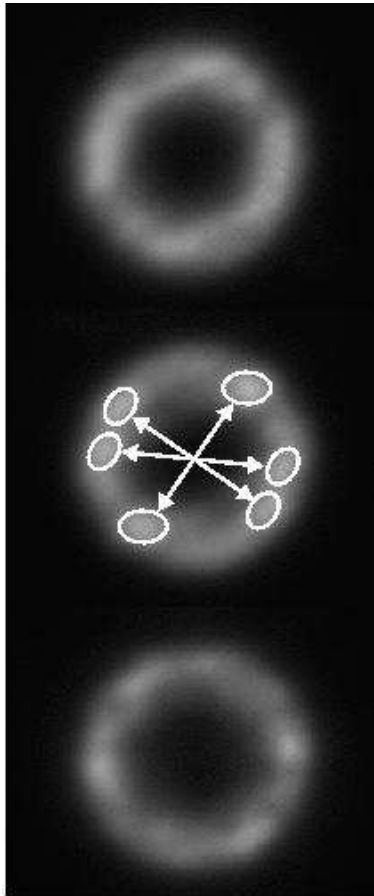


Fig.4 (b) Experimental observations by Devaud and Lantz at University of Besancon (see [12]).

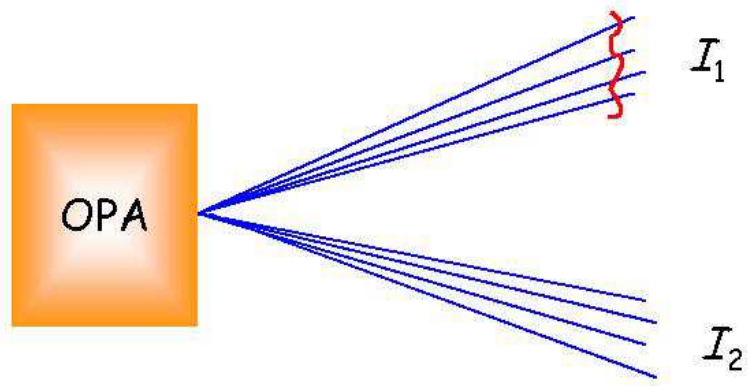


Fig.5. Detection of a weak amplitude object by measuring the intensity difference $i_1 - i_2$.

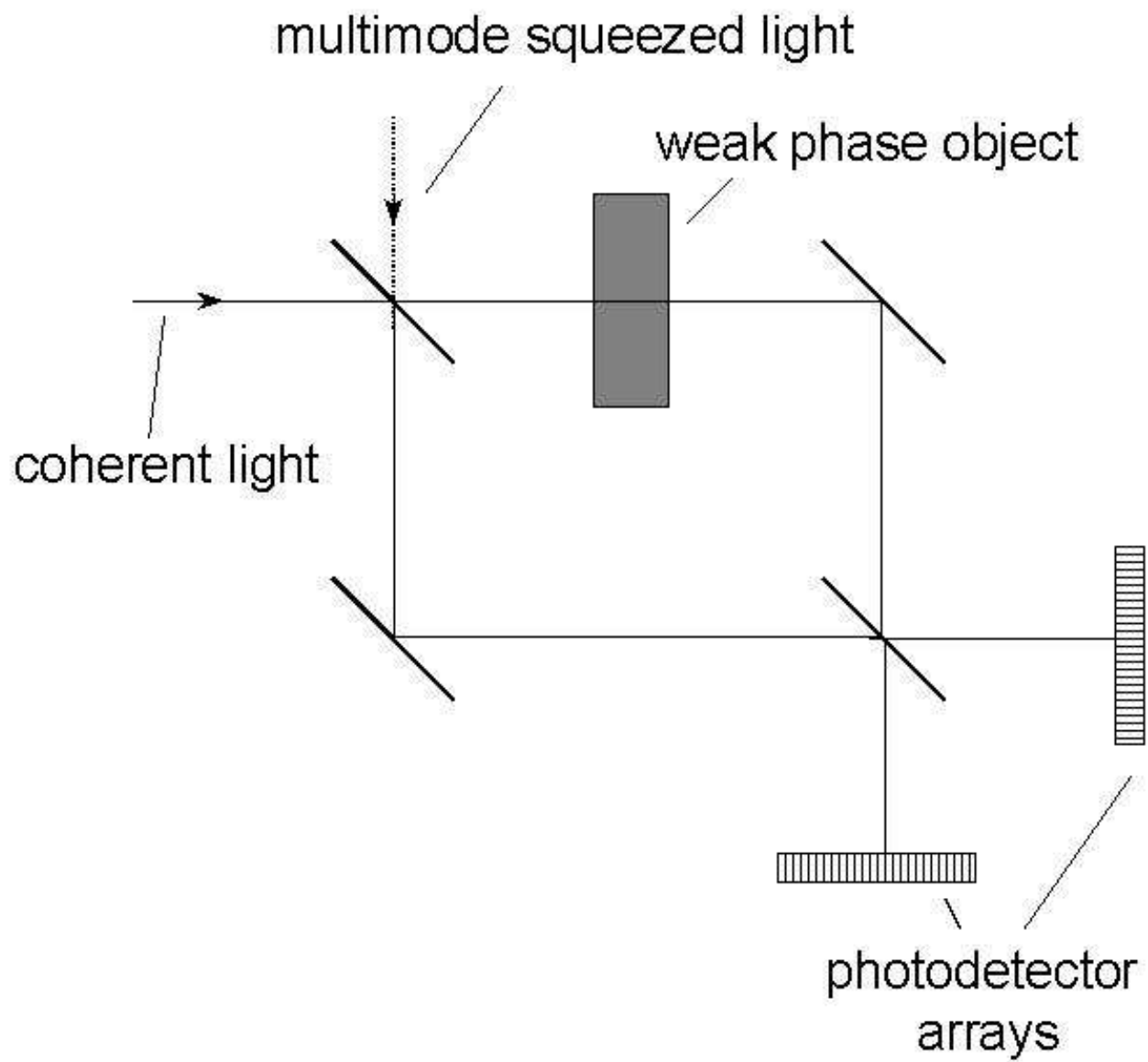


Fig.6. Detection of a weak phase object.

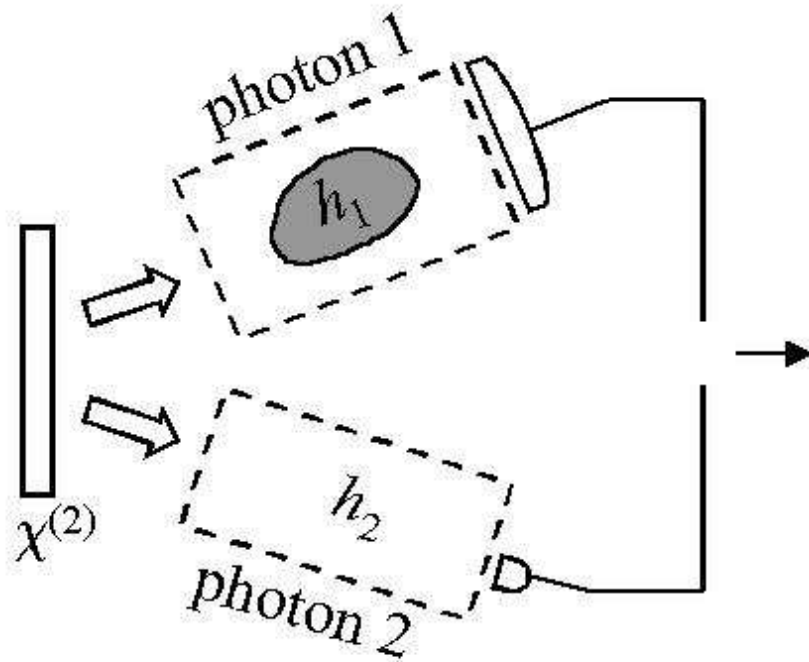


Fig.7 . Quantum imaging with entangled photon pairs. Photon 1 is revealed by a bucket detector which does not reveal its transverse position; photon 2 is observed by a detector that scans its position in coincidence with photon 1 detection.

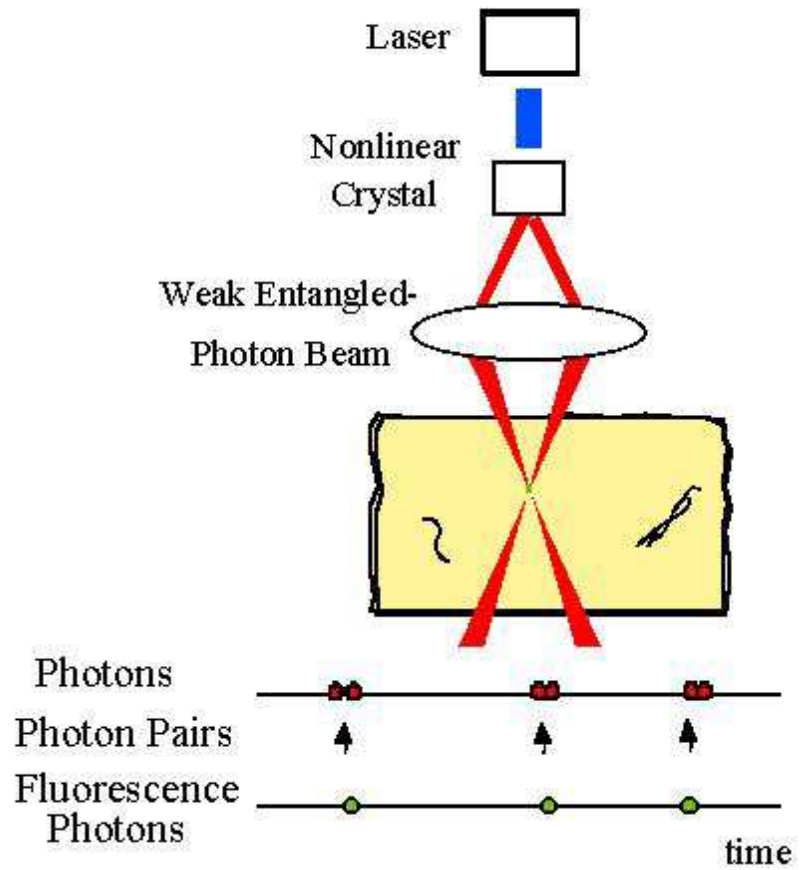


Fig.8 Illustration of entangled two photon microscopy.

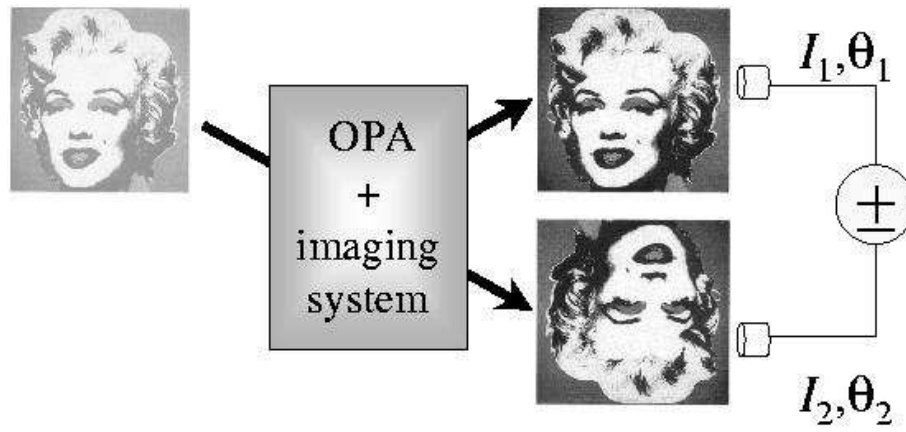


Fig.9. Off-axis injection of an image and generation of twin entangled images.

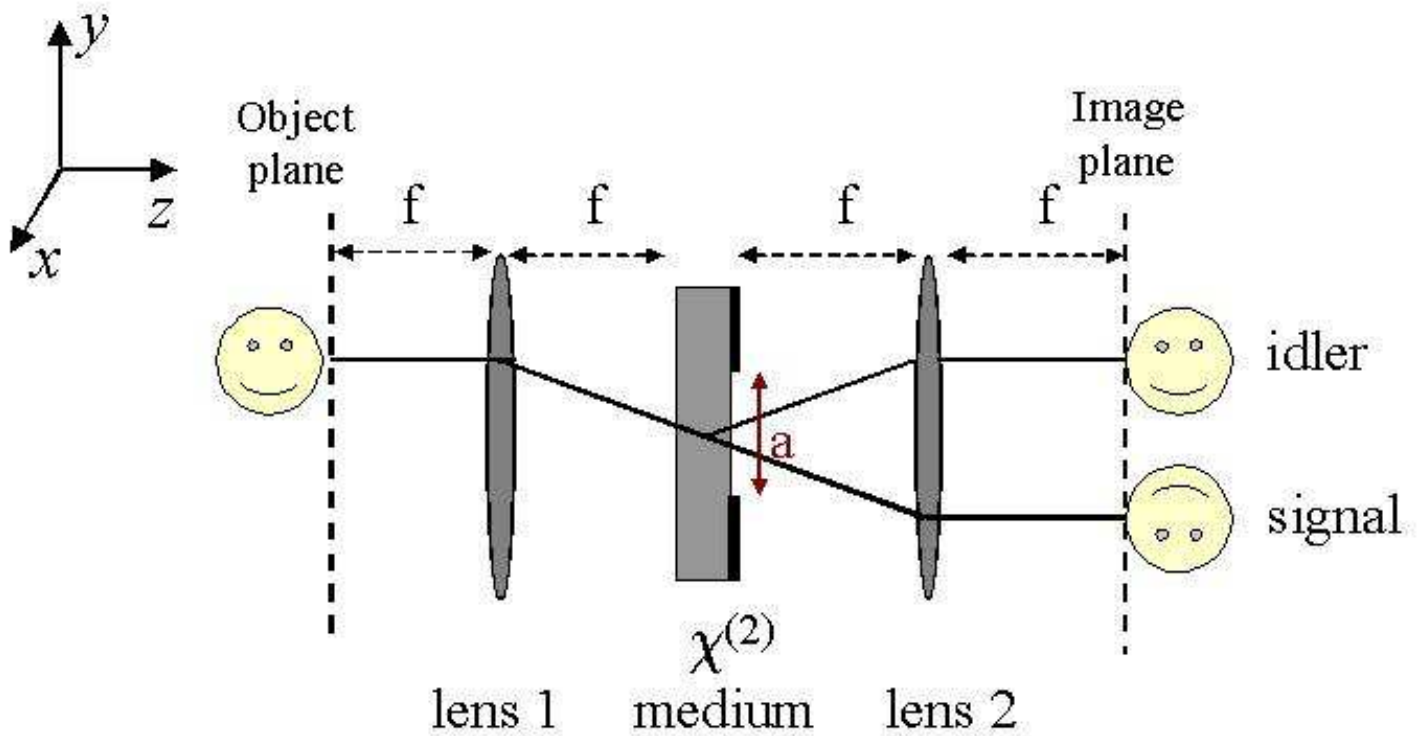


Fig.10. Scheme of the parametric optical image amplifier. Not shown in the figure is the pump field of frequency $2\omega_s$

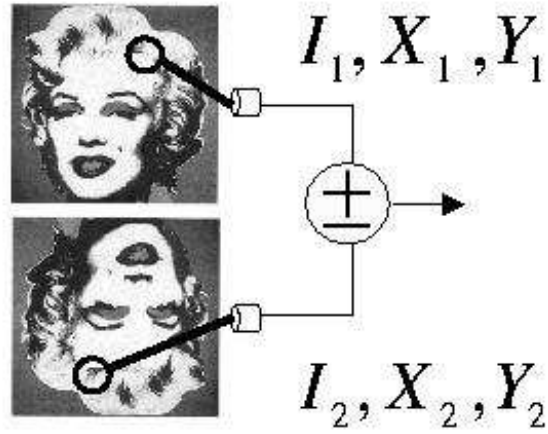


Fig.11. The spatial entanglement between the two output images concerns intensity and phase fluctuations, and also the fluctuations of quadrature components.



Fig.12. Analogy between the twin images and the two parts of a fossil.

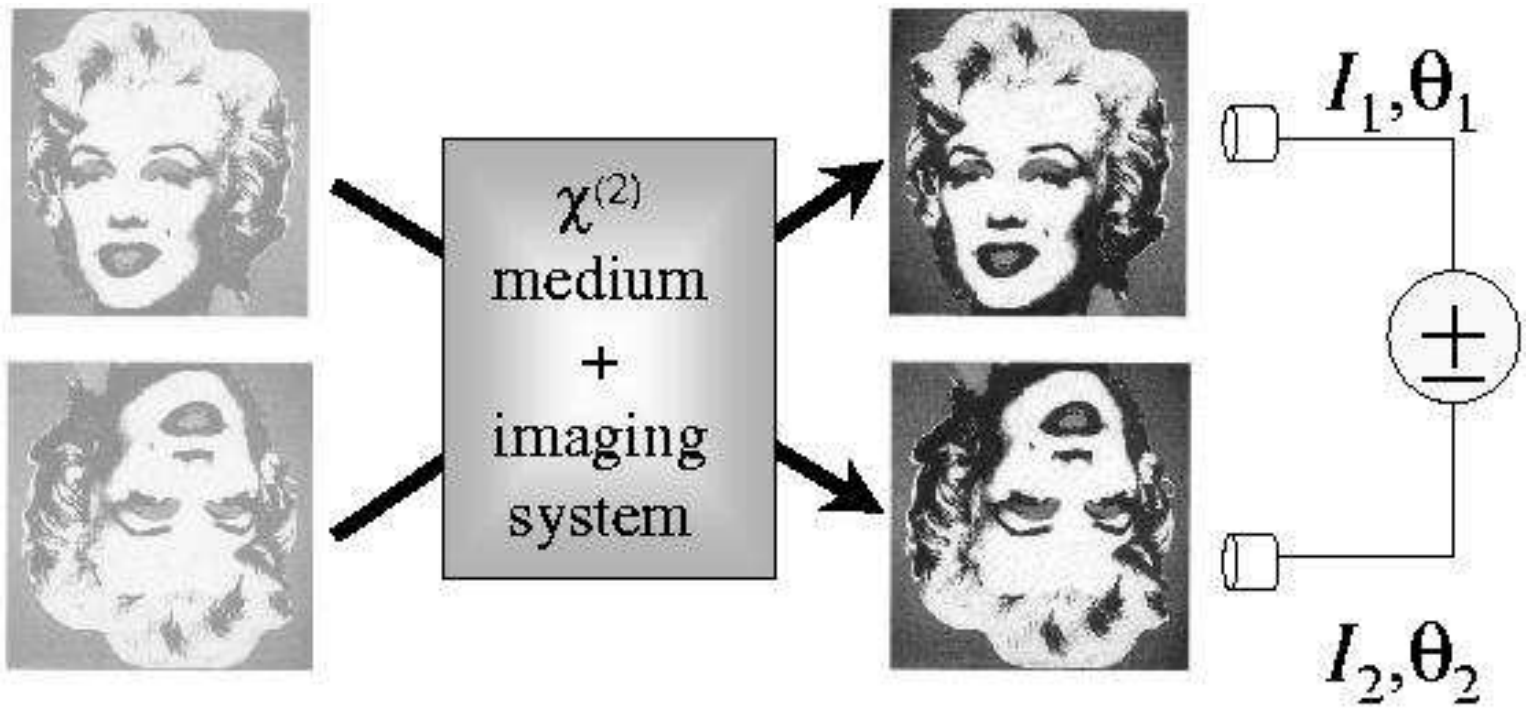


Fig.13. Symmetrical injection of an image.

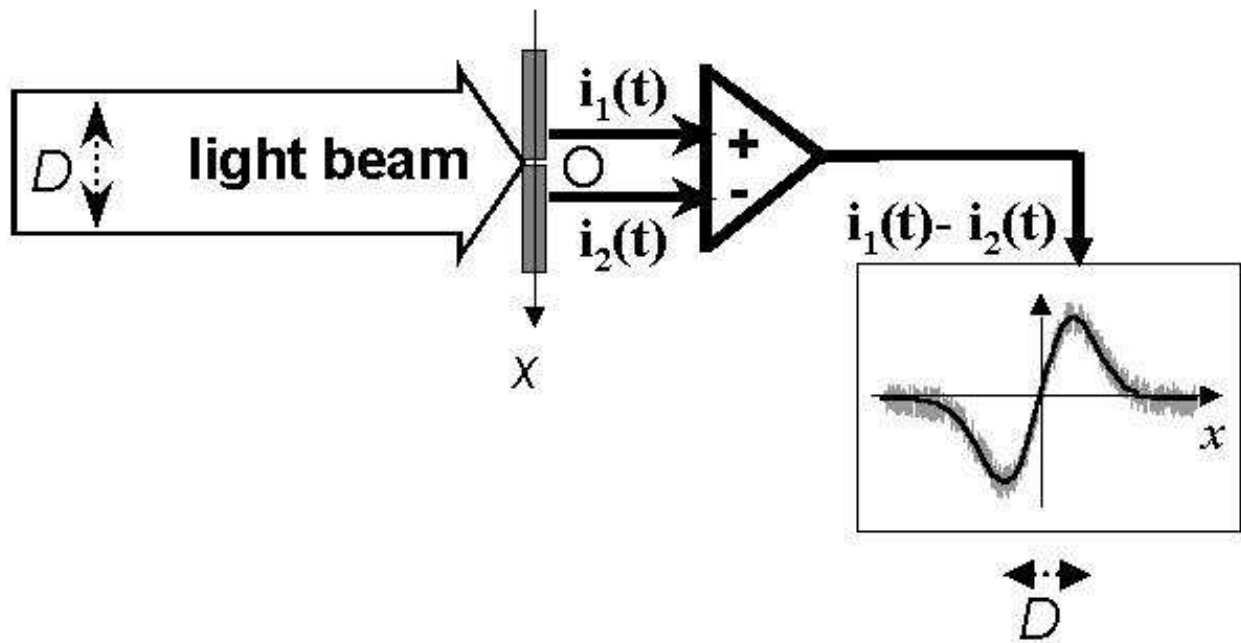


Fig.14. Measurement of very small beam displacements in the transverse plane.

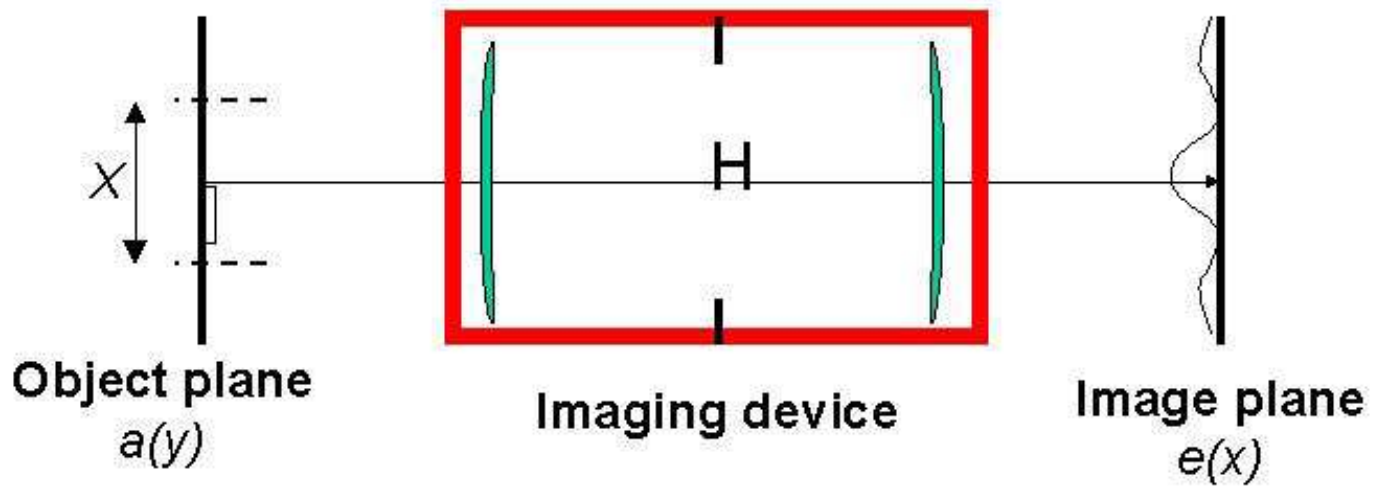


Fig.15. Scheme of the imaging system.

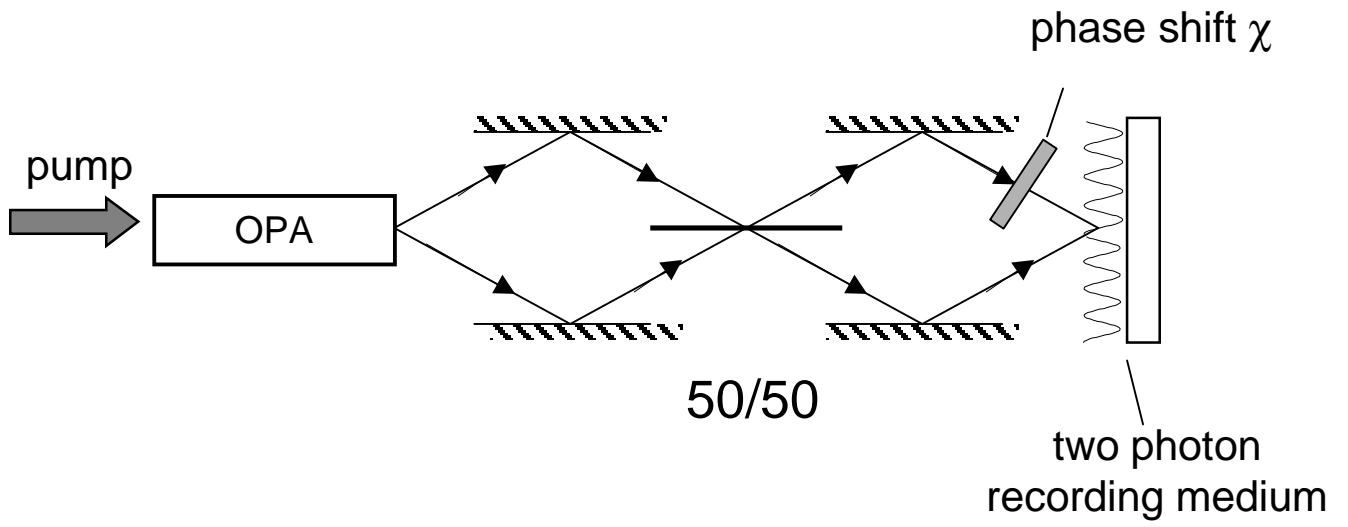


Fig.16. Scheme for quantum optical lithography.

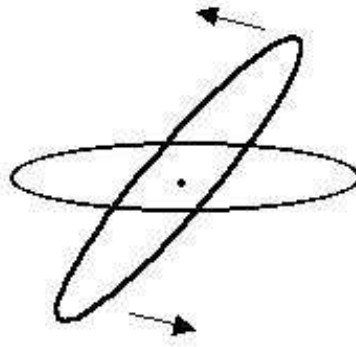


Fig.17. Interpretation of quantum lithography as interference between two squeezed vacuum beams.